

# Primary Intermediate in the Photocycle of a Blue-Light Sensory BLUF FAD-Protein, Tll0078, of *Thermosynechococcus elongatus* BP-1<sup>†</sup>

Yoshimasa Fukushima,<sup>‡,§</sup> Koji Okajima,<sup>‡,||</sup> Yutaka Shibata,<sup>§</sup> Masahiko Ikeuchi,<sup>||</sup> and Shigeru Itoh<sup>\*,§</sup>

Division of Material Science, Graduate School of Science, Nagoya University, Nagoya 464-8602, Japan, and Department of Life Science, Graduate School of Arts and Sciences, University of Tokyo, Tokyo 153-8902, Japan

Received September 10, 2004; Revised Manuscript Received February 7, 2005

**ABSTRACT:** Proteins with a BLUF (sensor of blue light using flavin adenine dinucleotide) domain represent a newly recognized class of photoreceptors that is widely distributed in the genomes of photosynthetic bacteria, cyanobacteria, and *Euglena*. Recently, Okajima et al. [Okajima, K., Yoshihara, S., Geng, X., Katayama, M. and Ikeuchi, M. (2003) *Plant Cell Physiol.* 44 (Suppl), 162] purified BLUF protein Tll0078 encoded in the genome of thermophilic cyanobacterium *Thermosynechococcus elongatus* BP-1 by expressing the protein in *Escherichia coli*. We investigated the photocycle of Tll0078 by measuring the picosecond fluorescence kinetics, transient absorption changes, and the UV–visible absorption spectra at 10 to 330 K. The absorption spectrum of the FAD moiety of Tll0078 showed a 10-nm red shift upon illumination at 278–330 K. The quantum efficiency of the formation of the red-shifted form was 29%. Illumination at 10 K, on the other hand, caused only a 5-nm red shift in about one-half of the protein population. The 5-nm-shifted form was stable at 10 K. The 5-nm red-shifted form was converted into the 10-nm red-shifted form at 50–240 K upon warming in the dark. At room temperature, the 10-nm red-shifted final product appeared within 10 ns after laser flash excitation. The lifetime of the fluorescence of FAD was found to be 120 ps at room temperature. These results reveal a fast and efficient photoconversion process from the singlet-excited state to the final product at room temperature. A photocycle of BLUF protein is proposed that includes the 5-nm red-shifted intermediate form as the precursor for the 10-nm red-shifted final product. The temperature dependence of each step of the photocycle is also discussed.

Recent genomic and physiological studies revealed new types of blue light sensing protein families that use flavin chromophores in the signal transduction (for review, see refs 1–4). Phototropin and cryptochrome found in plants and algae contain flavin chromophores that bleach upon absorption of light and trigger changes in the protein structure linked to the signal transduction cascade (5). On the other hand, a flavin adenine dinucleotide (FAD)<sup>1</sup> chromophore in AppA protein in a purple photosynthetic bacterium *Rhodospirillum rubrum* exhibits only a shift of the absorption band upon illumination (4). AppA has low homology with other flavoproteins in its amino acid sequence. It functions as the antirepressor of the transcription of photosynthetic genes in response to the blue light, or to oxygen concentration sensed by its –SH groups (4, 6–9). The absorption band of the FAD chromophore of AppA shifts 10 nm toward the red under illumination (4). This photoproduct is rather stable:

it takes more than 30 min to fully recover to the dark-adapted state again. Kraft et al. produced a photoinactive Y21F mutant type of AppA in which the Tyr21 residue is converted into Phe (10), and estimated the light-induced conformational changes in the FAD-surrounding moiety of the wild-type protein. The stronger H-bonding at the N5 position of the isoalloxazine ring was assumed to induce the red shift of FAD (10). NMR spectroscopy of the wild-type and Y21F proteins also suggested the  $\pi$ – $\pi$  stacking interaction of Tyr21 residue with the isoalloxazine ring of FAD (10). The FTIR spectroscopy of AppA revealed the light-induced change of the C(4)=O bond strength of the isoalloxazine ring and structural change of protein backbone (11, 12).

The amino acid sequence of AppA is composed of two domains: (i) the amino-terminal domain of about 17 kDa, which binds FAD noncovalently, and (ii) the carboxyl-terminal domain of about 31 kDa, which is rich in cysteine residues. The N-terminal domain seems to be the primary photosensing domain that triggers the conformational change and transmits the light signal to the C-terminal domain (4, 13). The gene regions encoding the FAD-binding domains were named “sensor of blue light using FAD (BLUF)” domains (14) that are widely distributed among genomes of photosynthetic bacteria, cyanobacteria, and *Euglena* (14, 15), although the cysteine-rich carboxyl domains are missing in most cases. The BLUF domains (without cysteine-rich C-terminal domains) were identified in the tll0078 gene of the thermophilic cyanobacterium *Thermosynechococcus elongatus* BP-1.

<sup>†</sup> This work was supported by a grant-in-aid (No. 15370067) and the COE program for “the origin of the universe and matter” from the Japanese Ministry of Education, Science, Sports and Culture.

<sup>\*</sup> To whom correspondence should be addressed. Phone: +81(52) 789 2881. Fax: +81(52) 789 2883. E-mail: itoh@bio.phys.nagoya-u.ac.jp.

<sup>‡</sup> The first two authors contributed equally to this work and are the primary coauthors.

<sup>§</sup> Division of Material Science (Physics), Graduate School of Science, Nagoya University.

<sup>||</sup> Department of Life Science, Tokyo University.

<sup>1</sup> Abbreviations: BLUF, sensor of blue-light using FAD; FAD, flavin adenine dinucleotide.

*gatus* BP-1 and the *slr1694* gene of the cyanobacterium *Synechocystis* sp. PCC6803, as well. The deletion mutant of *slr1694* of *Synechocystis* showed negative phototaxis to the white light in contrast to the positive phototaxis detected in the wild-type strain, implying the regulation of phototaxis by this protein (16, 17). Okajima et al. expressed the *tl10078* gene in *E. coli* and purified its gene product (16). The purified Tl10078 protein exhibited a 10-nm red shift of the absorption band of FAD upon illumination at room temperature, suggesting a photoreaction mechanism similar to that found in AppA, although Tl10078 lacks the cysteine-rich C-terminal domain. Masuda and Hasegawa investigated the photochemical reaction of the purified Slr1694 by FTIR spectroscopy (18, 19). They reported that light excitation weakened the C(4)=O and C(2)=O bonding of the isoalloxazine ring and strengthened the N1C10a and/or C4aN5 bonding.

Photoreceptor proteins, as bacteriorhodopsin, rhodopsin, or PYP, have been shown to attain the final signal-transducing states through multiple metastable intermediates. It is suggested that the small conformational change in the vicinities of the excited chromophore triggers the subsequent gross change of the whole protein structure (see refs 20 and 21). These intermediate states seem to be essential for the efficient photoreaction that leads to the conformational change of the protein.

The conserved amino acid sequences in the BLUF domains and the common photoproduct with its 10-nm red-shifted FAD absorption band in Tl10078, Slr1694, and AppA suggest a common mechanism in the primary photoevents, although Tl10078 has faster dark-recovery rates than AppA as shown in this study.

We investigated the intermediate states in the photocycle of Tl10078 protein by picosecond fluorescence decay measurements, nanosecond laser absorption spectroscopy, and static absorption spectroscopy at cryogenic temperatures. We have detected a new intermediate state that can be trapped only below 50 K. The mechanism and the energetics of the photocycle of the blue light sensory FAD protein Tl10078 will be discussed.

## MATERIALS AND METHODS

**Cloning, Expression, and Purification of Tl10078 Protein.** The entire coding region of Tl10078 of *T. elongatus* BP-1 was amplified from the genomic DNA by PCR with primers (5'-ACATATGGGACTACATCGCCTG-3' and 5'-CAGATC-TAGGATCCTTGACTCA-3'), which were designed to contain *Nde*I and *Bgl*III sites. PCR was performed with *Pfu* DNA polymerase (Stratagene, West Cedar Creek), and PCR products were cloned into the *Srf*I-digested pPCR-Script (Stratagene, West Cedar Creek) with XL10 cells according to the manufacturer's instructions. The DNA sequence was confirmed by the Big Dye terminator fluorescence detection method (Applied Biosystems, Foster City) with a capillary sequencer (PRISM 310 Genetic Analyzer, Applied Biosystems, Foster City). The sequenced DNAs were excised with *Nde*I and *Bgl*III and inserted into pET3xb (22).

Tl10078 protein was expressed in *E. coli* BL21 (DE3) pLysS transformed with the recombinant plasmids without the addition of IPTG. In principle, the Tl10078 protein should be expressed in *E. coli* BL21 (DE3) pLysS with IPTG.

However, in this case, the expression was not regulated by pLys and the protein could be expressed without IPTG. Upon the addition of IPTG, the protein was overexpressed, causing an increase of the inclusion body; therefore the protein expressed without IPTG was used for the purification. Cells were harvested after growth in an LB medium containing 40  $\mu\text{g mL}^{-1}$  ampicillin for 24 h at 25 °C. The harvested cells were suspended in a 20 mM Tris-HCl buffer (pH 7.5) containing 500 mM NaCl and 10 mM dithiothreitol and disrupted by sonication. The crude cell extract was centrifuged at 48000g for 60 min at 4 °C, and the supernatant was precipitated with 45% saturated ammonium sulfate. The precipitate was collected by centrifugation at 15000g for 30 min, dispersed in the same buffer, and subjected to size exclusion chromatography (Superdex 200 pg, Amersham Biosciences, Uppsala, Sweden). Fractions containing Tl10078 were collected, and the medium was exchanged to a 20 mM Tris-HCl buffer (pH 7.5) containing 100 mM NaCl and 10 mM dithiothreitol. The sample was applied onto an anion-exchange column (MonoQ HR 5/5, Amersham Biosciences, Uppsala, Sweden). Tl10078 protein was eluted with a 100–280 mM linear gradient of NaCl. Purified Tl10078 protein was concentrated to  $\sim 2 \text{ mg mL}^{-1}$  in 20 mM Tris-HCl buffer (pH 7.5) containing 1 M NaCl and 10 mM dithiothreitol. Purified BLUF protein was dissolved in a reaction medium containing 20 mM Tris-HCl buffer (pH 6.5) and stored at 5 °C until use.

**Measurement of the Absorption Changes Induced by Continuous 405-nm Diode Laser Light.** UV–visible absorption spectra were measured with a split beam double-monochromator spectrophotometer (Shimadzu UV-3100PC, Kyoto, Japan). The purified BLUF proteins were dissolved in a reaction medium containing 20 mM Tris-HCl (pH 6.5), 1 M NaCl, and 10 mM dithiothreitol. The sample was transferred to a quartz cuvette (optical path length of 10 mm) and was excited at 90° with a focused light from a continuous 405-nm CW laser diode (MLXF-A16-405-30; Kikogiken, Nishinomiya, Japan) at an intensity of 1900  $\mu\text{mol m}^{-2} \text{ s}^{-1}$  at the cuvette surface. In the measurements between 278 and 323 K, the temperature of the sample was controlled by circulating thermostated water. The wavelength resolution of the spectrograph was set at 5 nm, and the time courses of the absorption change upon the laser excitation were recorded with a time constant of 0.1 s.

The absorption spectra at low temperature were measured in a flow-type liquid-helium cryostat (CF1204DEG; Oxford Instruments, Oxford, U.K.) in combination with a temperature controller (ITC4; Oxford Instruments, Oxford, U.K.). For low-temperature measurements, glycerol was added to the reaction medium up to a final concentration of 63% (v/v), and then 500  $\mu\text{L}$  of a reaction medium in an acrylic cuvette (optical path length, 10 mm) was put into the cryostat and cooled to the desired temperatures.

**Measurement of Nanosecond Time-Resolved Absorption Spectra after 10-ns Laser Excitation at Room Temperature.** The time-resolved difference absorption spectra after 10-ns laser excitation were measured at 293 K with a home-built spectrophotometer consisting of a monochromator (MS257; ORIEL, Stratford), a cooled-CCD detector coupled with a gated image intensifier (Instaspec V ICCD detector Model 77193-5; ORIEL, Stratford), and a Xe flash lamp (SL-230S; Sugawara Laboratories Inc., Kawasaki, Japan). The image

intensifier was activated for 60 ns overlapping with the measuring Xe flash time profile at the desired delay time after the 10-ns excitation with a third harmonic (355 nm, pulse intensity close to 10 mJ) of a Nd:YAG laser (Quanta-Ray LAB-130-10TH; Spectra-Physics, Mountain View). The laser excitation was performed at a repetition rate of 0.05 Hz to minimize the accumulation of photoproduct during repeated excitations. The delay between the excitation and detection was controlled with a delay generator (DG535; Stanford Research System, California). Transient absorption spectra were accumulated from 30–90 times excitations at one delay time depending upon the desired signal-to-noise ratio. In the measurement of the absorption change at 10 ns, the contributions of the fluorescence excited by the actinic laser flash were subtracted. In these experiments, the reaction medium was the same as in the 405-nm excited continuous absorption measurements; the maximal absorbance of the Tl10078 protein was 1.7 at a 438-nm peak.

**Measurements of Fluorescence Lifetime.** The fluorescence decay at 293 K was measured with a set of monochromator (Chromex 2501-S; Hamamatsu Photonics, Hamamatsu, Japan) and a streak-camera (4334; Hamamatsu Photonics, Hamamatsu, Japan) coupled to a CCD detector. Fluorescence excited by a pulsed laser diode (405 nm, pulse width 50 ps, at a repetition rate of 1 MHz and at an intensity of  $7 \mu\text{mol m}^{-2} \text{s}^{-1}$ , Hamamatsu Photonics, Hamamatsu, Japan) was focused through a long-pass filter (Y-43, Toshiba, Tokyo) onto the entrance slit of the spectrograph. After dispersion of light as a function of wavelength in the monochromator (x-axis later in the image), each photon at a different wavelength was transformed into a bunch of electrons in the image intensifier placed at the entrance of the streak-camera, and was recorded as a function of arrival time (y-axis later in the image) by the streak-camera. The CCD camera set at the exit of the streak-camera detected each bunch of electrons at its corresponding  $x$ - $y$  (wavelength–time) position. The CCD-image was transferred to a computer, and a central  $x$ - $y$  location in each bunch of electrons was recorded as the point of each photon in the wavelength–time two-dimensional space. The data points were accumulated with a 10-ns time window. BLUF proteins in the same reaction medium as in the absorption measurements were put into a 10-mm quartz cuvette and were stirred during the measurement.

The excitation beam was focused onto the surface of the sample cuvette in a spot with a diameter of  $\sim 1$  mm to give the number of photons in a single laser excitation to be  $\sim 10^{-17}$  mol, which is far less than the number of flavin molecules ( $\sim 10^{-9}$  mol) in an excitation volume of  $\sim 1 \mu\text{L}$ . Therefore, the double or triple excitations of the same molecule by the laser pulse seemed negligible. The amount of the photoproduct accumulated per unit of time, on the other hand, can be estimated to be less than  $\sim 10^{-11}$  mol/s ( $\sim 10^{-17}$  mol in a single pulse at 1 MHz), and that of the FAD molecules in the sample,  $\sim 10^{-7}$  mol. With the observed recovery rate of 17 s at 293 K (see Results), the amount of the photoproduct accumulated during the fluorescence measurement, therefore, could be negligible.

## RESULTS

**The Light-Induced Absorption Change of BLUF Protein.** Dark-adapted Tl10078 protein at room temperature showed

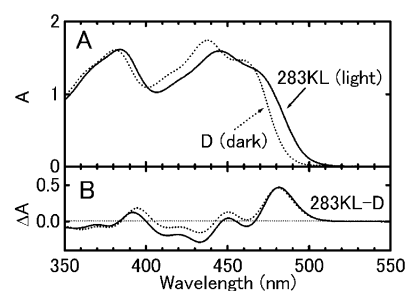


FIGURE 1: (A) Effect of illumination on the absorption spectrum of purified Tl10078 protein at 284 K: (···, dotted line) dark-adapted absorption; (—, solid line) light-adapted (405 nm,  $1900 \mu\text{mol m}^{-2} \text{s}^{-1}$ ) absorption. (B) Light-minus-dark difference spectrum (—) and simulated difference spectrum (···). The simulated difference spectrum is the difference between the 10-nm red-shifted dark-adapted and the original dark-adapted spectra as described in text.

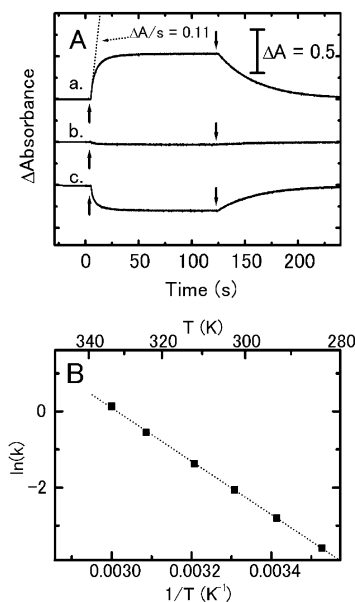


FIGURE 2: (A) The time-course of the absorbance change at 284 K measured at 482 nm (a), 466 nm (b) or 433 nm (c). The broken line in trace a shows the initial rate of the light-induced absorption change. (B) Arrhenius plot of the dark-recovery rate of the absorption change of the Tl10078 protein between 284 and 333 K. The dark-recovery rate after 1–3 min of continuous illumination was measured, as shown in Figure 2A trace a for 482 nm.

absorption peaks and shoulders at 467.2, 437.4, 414.4, 382.8, and 362.4 nm at 284 K (Figure 1A, dotted line). Upon the illumination of 405-nm blue laser light, the spectrum changed significantly, giving a new absorption band around 480 nm (Figure 1A, solid line). The light-minus-dark difference spectrum indicated positive (+) and negative (−) peaks at 481.8 nm (+), 461.4 nm (−), 451.0 nm (+), 432.8 nm (−), 418.6 nm (+), 413.2 nm (−), and 391.8 nm (+) as shown by a solid line in Figure 1B. The difference spectrum can be interpreted as a  $510\text{-cm}^{-1}$  (10-nm) red shift of the whole spectrum after the simple simulation. We replotted the spectrum against the wavenumber and shifted to the lower-energy side by  $510 \text{ cm}^{-1}$  to fit to the spectrum under illumination as shown by a dotted line in Figure 1B.

Figure 2A shows the time courses of the absorption change at 284 K upon the laser illumination. Upon laser excitation, the time course showed changes that were positive, nonexistent, and negative, respectively, at 482, 466, and 433 nm, at which wavelengths the difference spectrum in Figure 1



showed a positive peak, an isosbestic point, and a negative peak. The extent of absorbance change attained its maximum after 50 s of illumination at a laser intensity of  $1900 \mu\text{mol m}^{-2} \text{s}^{-1}$ . Upon the offset of the laser light, the light-adapted state relaxed with an apparent half-time of 25 s in each case. The apparent dark-recovery rate constant was calculated to be  $0.03 \text{ s}^{-1}$  ( $\tau_{1/e} = 36.2 \text{ s}$ ) by assuming a single-exponential decay. Similar time courses were measured between 278 and 333 K at 483 nm to study the temperature dependency of the dark-recovery rate. At the lower temperatures, the rising rate upon illumination decreased slightly (not shown), while the relaxation rate of the light-adapted state to dark decreased significantly. The logarithm of the time constants (obtained by assuming single-exponential decays) of the light-adapted state relaxation were plotted against the inverse of the temperature in Figure 2B. This Arrhenius plot gave a straight line, leading to an activation enthalpy of 0.61 eV (59 kJ mol<sup>-1</sup>) and to an activation entropy of  $-7.2 \times 10^{-4} \text{ eV K}^{-1}$  ( $-69 \text{ J mol}^{-1} \text{K}^{-1}$ ). These values give an activation free energy value of  $\Delta G^\ddagger = 0.84 \text{ eV}$  (81 kJ mol<sup>-1</sup>) at 324 K. The high  $\Delta G^\ddagger$  value suggests some changes in the protein structure during the dark recovery (10, 12, 18, 19, 23).

The apparent quantum efficiency of the photoconversion was calculated on the basis of the absorption cross section of FAD by assuming that FAD in the BLUF protein has the same absorption coefficient at 438 nm ( $\epsilon_{438}^{\text{dark}}$ ) of  $8300 \text{ cm}^{-1} \text{mol}^{-1}$  as in AppA (10). The time course of the absorption change at 483 nm showed an initial rise rate of  $0.11 \pm 0.01$  ( $\Delta\text{OD s}^{-1}$ ) (Figure 2A, dashed line). The molar absorption coefficient at 483 nm of the dark form  $\epsilon_{483}^{\text{dark}}$  was estimated to be  $1600 \text{ cm}^{-1} \text{M}^{-1}$  by comparing the optical density at 438 and 483 nm in the absorption spectrum of the dark form. The molar absorption coefficient at 483 nm of the photo-product  $\epsilon_{483}^{\text{light}}$  was also calculated to be  $5000 \text{ cm}^{-1} \text{M}^{-1}$  by shifting the absorption spectrum of dark form to the red by  $510 \text{ cm}^{-1}$  and by assuming a slight decrease of the molar absorption coefficient (with a factor of 0.94) in the photo-product (see the section "Temperature Dependence of the Conversion from the I to the F Forms"). With these values, a difference molar absorption coefficient of the photo-conversion for 483 nm ( $\Delta\epsilon_{483}$ ) can be calculated to be  $\Delta\epsilon_{483} = \epsilon_{483}^{\text{light}} - \epsilon_{483}^{\text{dark}} = 3400 \text{ cm}^{-1} \text{M}^{-1}$ . Therefore, the amount of the molecules involved in the photocycle per second in the initial phase of the photoconversion was calculated to be  $10 \pm 1 \text{ nmol s}^{-1}$ . On the other hand, the photon flux absorbed by FAD in this experiment at 405 nm at the laser intensity of  $1900 \mu\text{mol m}^{-2} \text{s}^{-1}$  corresponds to  $35 \text{ nmol s}^{-1}$ . Thus, the quantum efficiency of the photoconversion is  $29 \pm 3\%$ , which indicates that the efficiency of the photo-conversion is high at physiological temperatures.

The time constant of the recovery of the dark-adapted form from the photoconverted form of the TlI0078 protein (at 324 K, where *T. elongatus* was grown) was rather fast ( $1.74 \text{ s}^{-1}$ ). This recovery rate is about 700–800 times faster than the dark-recovery rate of the light-adapted form of AppA, which gives a  $\tau_{1/e} \sim 20 \text{ min}^{-1}$ , measured at room temperature (close to the growth temperature of *Rb. sphaeroides*) (4). Full recovery of the absorption change in AppA was reported to require dark time of over 30 min (4), while the 1-min dark time was sufficient for the full recovery of TlI0078 protein even at room temperature, indicating the faster recovery of the latter.

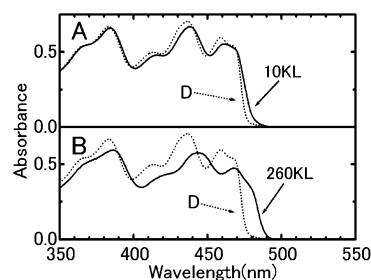


FIGURE 3: Absorption spectra of the TlI0078 protein taken at 10 K. The dotted lines in panels A and B represent the same absorption spectrum of the dark-adapted form (D sample). Solid line in panel A is the absorption spectrum of the TlI0078 protein, illuminated at 10 K (10KL sample). Solid line in panel B: illuminated at 260 K for 10 min and kept under light during cooling to 10 K (260KL sample).

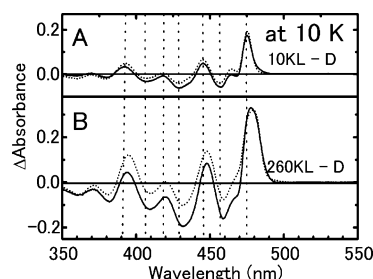


FIGURE 4: Difference absorption spectra of the TlI0078 protein measured at 10 K. (A) The solid line shows the difference between 10KL and D spectra (for the original spectra, see Figure 3A). The dotted line is a simulated spectrum obtained as difference between the 5-nm ( $230\text{-cm}^{-1}$ ) red-shifted-dark D spectrum and the original D form spectrum. (B) The solid line is the difference between the spectra 260KL and D (for the original spectra, see Figure 3B). The dotted line is a simulated spectrum obtained as difference between the 10-nm ( $510\text{-cm}^{-1}$ ) red-shifted D spectrum and the original D spectrum.

**The Intermediate State Trapped at Low Temperature.** For these measurements, glycerol was added to the protein solution to form a transparent ice and the sample was frozen in the dark (D sample). The spectrum at 10 K of the D sample showed peaks and shoulders at 470.2, 458.4, 439.2, 430.8, 412.6, 384.6, and 363.0 nm (dotted lines in Figure 3 A,B). At 10 K, all bands were narrower than at room temperature, indicating significant decrease of the molecular motions.

After illumination of the D sample at 10 K, the absorption spectrum shifted toward the red (solid line in Figure 3A). The absorption change saturated after 15-min illumination (not shown), indicating a slower photoconversion at 10 K as compared to that at 284 K (there the saturation time was 50 s). The light-minus-dark difference spectrum at 10 K (difference between the solid and dotted lines in Figure 3A) indicated positive peaks at 475.2, 464.8, 445.6, 418.8, and 392.4 nm and negative peaks at 468.0, 457.6, 429.0, and 406.8 nm (solid line in Figure 4A). The difference spectrum can be simulated as a  $230\text{-cm}^{-1}$  (about 5 nm but not 10 nm) red shift of the dark spectrum (a dotted line in Figure 4A). The spectral feature of the 10KL sample did not change even after 30-min illumination, and the 10KL spectrum could not be converted back to the spectrum of D sample in the dark.

We illuminated the dark-adapted TlI0078 protein at 260 K to fully convert to the 10-nm red-shifted form, and then cooled it to 10 K under continuous illumination (260KL sample). The absorption spectrum of the 260KL sample gave a marked shoulder at 481.0 nm, which was undetectable

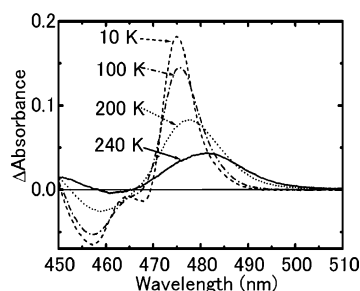


FIGURE 5: Temperature-dependent change of the light-minus-dark difference absorption spectrum of the Tll0078 protein. The absorption spectrum of the dark-adapted sample (D sample) was recorded each 10 K during slow cooling to 10 K at a rate of 2 K/min in the dark. On cooling to 10 K, the sample was illuminated with a 405-nm laser light for 10 min (10KL sample), and the absorption spectra were then measured each 10 K during warming up in the dark at a rate of 1.5 K/min. The difference spectra between the 10KL and D samples were then calculated from a set of spectra measured at 10, 100, 200, and 240 K, respectively, as indicated in the figure.

either in the D sample or in the 10KL sample (solid line in Figure 3B). The difference spectrum at 10 K of the 260KL sample minus the D sample showed positive peaks at 477.6, 448.0, 420.2, and 394.0 nm and negative peaks at 458.8, 431.2, and 409.0 nm (solid line in Figure 4B). This difference spectrum can be simulated by assuming the  $510\text{-cm}^{-1}$  (10 nm) red shift of the spectrum of D sample (dotted line in Figure 4B) as it was found in the room-temperature experiment (Figure 1 inset). Thus, the 10KL sample and the 260KL sample must represent different intermediates of the photocycle. Each peak in the 260KL-minus-D difference spectrum is at 2–3 nm longer wavelengths than those in the 10KL – D difference spectrum (Figure 4). Although the 260KL – D difference spectrum showed a small blue shift and band narrowing on cooling from 260 to 10 K, it was clearly different from the 10KL – D difference spectrum. The illumination at 260 K induces a  $510\text{-cm}^{-1}$  (10-nm) red shift, while the illumination at 10 K induces only a  $230\text{-cm}^{-1}$  (5-nm) red shift. Thus, we detected three forms of the protein at 10 K, a dark-adapted form of D sample (D form), a 5-nm red-shifted form in the 10KL sample (I form), and a 10-nm red-shifted form in the 260KL sample (F form).

**Transition from the I to the F Form by Warming.** In order to investigate the relation between the photoevents at 10 K and higher temperatures, we examined the effect of warming on I form in the dark. The 10KL sample (I form) was warmed up to designated temperature in the dark, and the absorption spectra were measured at each temperature. No significant change in the spectral shape was detected in the difference spectrum of the I form that was warmed to 100 K: the peak heights decreased due to the slight broadening of the bandwidths with slight shifts of the peak positions (Figure 5). At 200 K the peak positions shifted drastically to the longer wavelengths. At 240 K, the peak positions of the difference spectrum coincided with the peak positions of the F form of 260KL minus D samples measured at 240 K. The result indicates that the I form accumulated at 10 K is stable until 100–200 K and was converted into the F form, which is identical to the one formed by illumination at the higher physiologically relevant temperatures. The I form, thus, seems to be an intermediate to produce the F form (or an intermediate in the side path). It is also suggested that the formation of the I form appears to require only a slight

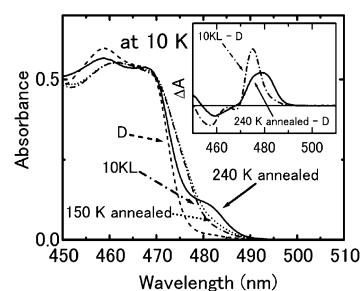


FIGURE 6: Absorption spectra at 10 K of the Tll0078 protein after illumination at 10 K and after annealing treatments at higher temperatures. The protein solution frozen in the dark was illuminated at 10 K, annealed at either 150 or 240 K in the dark for more than 20 min, and then cooled down to 10 K in the dark to measure the spectrum at 10 K again. Broken (---) and chain lines (— · —): absorption spectra of the dark-adapted and 10 K-illuminated samples, respectively. Dotted (···) and solid lines (—): absorption spectra of the 10 K-illuminated sample after annealing at 150 and 240 K, respectively. Inset: Difference spectrum between the 10 K-illuminated and the dark-adapted sample (10KL – D, chain line (— · —)) and that between the 10 K spectra after being annealed at 240 K for 20 min and the dark-adapted sample (240 K annealed – D, solid line).

modification of the molecular coordinates that are available even at 10 K. The I form seems to change into the F form, with the larger change in molecular structure that is available only above 200 K.

**Temperature Dependence of the Conversion from the I to the F Forms.** To investigate the temperature dependence of the conversion process from the I to the F form, the spectrum of the 10KL sample was measured at 10 K after a dark-annealing treatment at different temperature. The 10KL sample (that shows the spectrum of I form) was warmed and maintained at 50 K for about 20 min and then cooled to 10 K again to measure the absorption spectrum. This type of dark annealing at 50 K modified the spectrum slightly. Similar annealing and cooling processes were repeated subsequently by changing the annealing temperatures to 100, 150, 200, and 240 K, respectively, and the absorption spectrum was then measured at 10 K as shown in Figure 6. The inset of Figure 6 represents the difference spectra of 10KL – D (I form) and 240K annealed – D (F form converted from I).

The spectrum of the sample annealed below 200 K showed a slight change as compared to that of the 10KL sample. However, the annealing at 240 K increased the intensity of the 482-nm band characteristic of the F form and decreased the 475-nm band characteristic of the I form. The increase of a peak at 458.8 nm, which was identical to the peak of the D form, was also detected. The difference between the 240 K annealed sample and the D sample showed a lower positive peak intensity around 480 nm. As shown in the difference spectrum in the inset of Figure 6, it is clear that the I form was converted into the F form by the thermal activation at 240 K. However, the lower height of the absorption around 475 nm of the whole spectrum of the 240 K annealed sample also suggests a partial decay to the D form.

We estimated the amounts of D form, I form, and F form after each annealing treatment by a simple spectrum-fitting program; each annealed absorption spectrum ( $S(\omega)$ ) recorded at 10 K was fitted with a linear combination of spectra of these three forms as follows. The spectra of the I and F forms

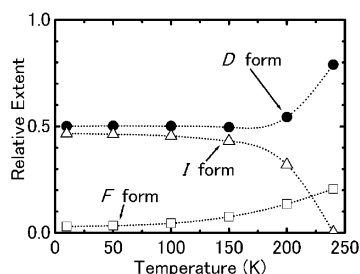


FIGURE 7: Estimated extents of the dark-adapted D form, 5-nm-shifted I form, and 10-nm-shifted F form after annealing treatments of the 10 K-illuminated Tl10078 protein. The extent of each form was estimated from the absorption spectrum obtained at 10 K after an annealing treatment at the designated temperatures by the curve-fitting simulation program, described in text.

were calculated by shifting the spectrum of the D form measured at 10 K with a slight modification of its molar extinction coefficient.

$$S(\omega) = c_D f_D(\omega) + c_I f_I(\omega) + c_F f_F(\omega) \\ \approx c_D f_D(\omega) + c_I \alpha f_D(\omega - 230 \text{ cm}^{-1}) + \\ c_F \beta f_D(\omega - 510 \text{ cm}^{-1})$$

where  $\omega$  represents the wavenumber and  $f_D(\omega)$ ,  $f_I(\omega)$ , and  $f_F(\omega)$  represent the absorption spectra of the D form, the 230- $\text{cm}^{-1}$  (5-nm)-shifted I form, and the 510- $\text{cm}^{-1}$  (10-nm)-shifted F form, respectively, at wavenumber  $\omega$ .  $c_D$ ,  $c_I$ , and  $c_F$  represent the relative concentrations of the D, I, and F forms, respectively.  $\alpha$  and  $\beta$  represent the relative changes of the molar extinction coefficient in the I and F forms with respect to that of the D form. Initially, a set of the  $c_D$ ,  $c_I \alpha$ , and  $c_F \beta$  values of each spectrum was determined by a fitting program by assuming simple spectral shifts. Then, the  $\alpha$  and  $\beta$  values were adjusted to give the sum of  $c_D$ ,  $c_I$ , and  $c_F$  to 1.0 in each spectrum. The values of  $\alpha$  and  $\beta$  of 0.93 and 0.94, respectively, gave the best fit to the experimental results.

The relative contributions of D, I, and F in the 10KL sample were calculated to be 0.50, 0.46, and 0.03, respectively, as shown in Figure 7. Only a half of the protein, therefore, seemed to be photoactive at 10 K to give I even under illumination at sufficient intensity and period. The result might represent the heterogeneity of D or some other unknown mechanism. After annealing at 10–150 K, a slight increase in F (from 0.03 to 0.08) and a decrease in I (from 0.47 to 0.43) were detected, indicating a partial conversion from I to F. Above 200 K, the extent of the conversion increased more significantly. The result suggests that I is the intermediate state in the photocycle of Tl10078 at low temperatures. In addition to the increase of the F form after annealing, the relative amount of the D form increased above 200 K. The I disappeared at 240 K annealing, indicating the full conversion to either F ( $c_F(240 \text{ K})/c_I(10 \text{ K}) = 0.20/0.47 = 42\%$ ) or D ( $100\% - 42\% = 58\%$ ). The high yield of D (58%) after annealing at 240 K is somewhat strange, since the F produced by the illumination at higher temperature practically cannot relax to D below 270 K due to the high activation energy barrier, as estimated in Figure 2B.

**Measurement of the Time-Resolved Absorption Spectra at Room Temperature after a 10-ns Laser Flash.** Figure 8 inset shows the transient difference absorption spectra of the

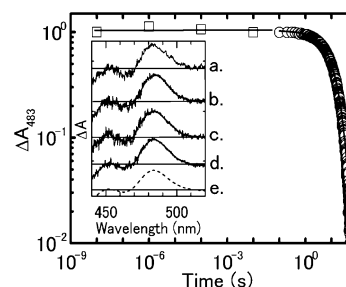


FIGURE 8: Formation and decay kinetics of the F form of the Tl10078 protein at room temperature. Squares represent the extents of the absorption change at 483 nm measured after 10-ns, 355-nm laser flash excitations as a function of time, calculated from the time-resolved difference spectra, as shown in the inset. Circles represent the dark decay time course of the absorption change at 483 nm measured continuously using a UV-3100 spectrophotometer after 1-min illumination at 405 nm, as shown in Figure 2. Both traces were normalized at the maximum. Inset: Time-resolved difference spectra of Tl10078 protein after the 355 nm laser excitation measured at delay times of 10 ns (a), 1  $\mu\text{s}$  (b), 100  $\mu\text{s}$  (c), and 10 ms (d). The broken line (e) shows the normalized light-minus-dark difference spectrum obtained under the continuous illumination of a 405-nm laser (at the intensity of  $1900 \mu\text{mol m}^{-2} \text{s}^{-1}$ ).

BLUF protein measured at delay times of 10 ns, 1  $\mu\text{s}$ , 100  $\mu\text{s}$ , and 10 ms after 10-ns laser excitation at 355 nm at room temperature. The repetition rate of the excitation laser flash was set to be very slow (at 0.05 Hz) to minimize the accumulation of I and F forms. The difference spectrum at a 10-ns delay time showed a positive peak at 483 nm, indicating the formation of F (traces a and e in Figure 8 inset). The I form was not detected, even at the shortest 10-ns delay time. The spectral shape was almost invariant from the 10-ns to 10-ms delay times and was almost the same as that measured under continuous illumination. Therefore, only F was detectable at 10 ns after laser excitation at room temperature in our measurement. The result confirms the fast rise kinetics ( $<1 \mu\text{s}$ ) of AppA protein measured by Kraft et al. (10). The spectral shifts disappeared within 1 min, as observed after continuous illumination. The photoconversion process of Tl10078, therefore, does not seem to include the long-lived triplet state of FAD. The result, however, does not exclude the possibility of participation of a triplet state with a lifetime shorter than 10 ns.

**Measurement of the Picosecond Fluorescence Decay.** The emission spectrum and the decay time course of the fluorescence of Tl10078 were measured at 290 K. The fluorescence spectrum showed a peak at 510 nm at any time range (Figure 9). The fluorescence decay was measured and simulated with three components with decay time constants (and relative initial extents) of 0.12 ns (0.95), 0.71 ns (0.04), and 4.56 ns (0.01), respectively. The emission from the photoaccumulated I and F may contribute, partially, to the fluorescence decay. However, their accumulation can be estimated to be less than 4% under the present experimental conditions; therefore, the measured lifetime mainly represents that of the laser-excited D. The slower fluorescence decay components that amount to 5% in initial extents might represent the inactive proteins.

The major component with a short decay time of 0.12 ns suggests that the initial photochemical event takes place in competition with the 0.12-ns emission process. The initial photoconversion process seems to occur from the singlet



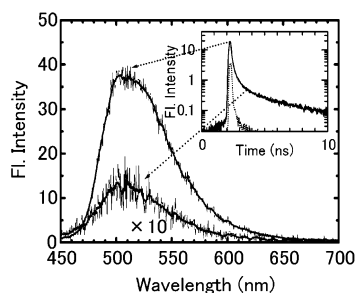


FIGURE 9: Time-resolved fluorescence spectra of the Tll0078 protein measured at 0.1 and 1.7 ns after a 50-ps-long, 405-nm laser excitation at room temperature. The amplitude of the spectrum taken at 1.7-ns delay was expanded 10-fold. Inset: Decay kinetics of the fluorescence calculated for the whole wavelength region (solid line). The dotted line represents the profile of the exciting laser pulse.

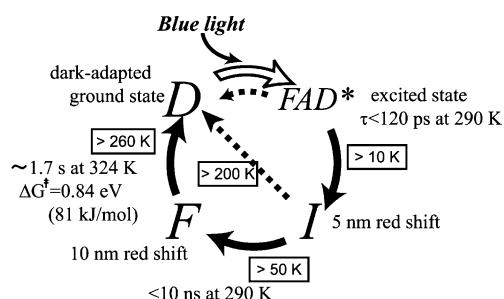


FIGURE 10: Proposed scheme of the photocycle of the Tll0078 protein based on the temperature dependences of the transitions between the different intermediates.

excited state of FAD. This result is consistent with that of time-resolved spectroscopy in Figure 8, which showed that the full extent of the F form was present at 10 ns after the laser excitation. Since no I was detected by time-resolved spectroscopy at room temperature, it is suggested that the primary photoevent occurs in competition with the fast 0.12-ns fluorescence emission and produces the F form within 10 ns. The I form, therefore, might exist between 0.12 and 10 ns if it is also formed at 290 K.

## DISCUSSION

**Photocycle of Tll0078 BLUF Protein Including the Intermediate State.** On the basis of the results obtained in the present study, we propose a reaction scheme in Figure 10. Tll0078 exhibits a photocycle that involves four forms, the dark-adapted form, the form with the excited state of FAD (FAD\*), the 5-nm red-shifted form, and the 10-nm red-shifted form. We abbreviate these forms as the D, FAD\*, I, and F forms, respectively. The transition from FAD\* to I will proceed in competition with the fluorescence emission process and will result in the 120-ps deactivation time of FAD\*. The mechanism for this step is interesting but not yet known. The I form is stable at 10 K and does not decay to D again below 200 K. The motions of the molecular coordinates in proteins are expected to be strictly limited at 10 K; therefore, the conformational change responsible for the 5-nm shift of the FAD spectrum seems to be limited inside FAD or in its close vicinity. This may be accomplished by a slight rearrangement of the atoms close to the FAD. The replacement of a proton, through a tunneling mechanism, from a side chain of an amino acid like an amide group to the C=O carbonyl of the isoalloxazine ring may affect its spectrum. The slight rearrangement may be required to

compensate for the abrupt change of the charge distribution upon the photoproduction of FAD\*, and the H-bond between the de-excited FAD and the side chain of the amino acid residue may be strengthened in the altered microenvironments.

The transition from the I to the F form occurs slightly above 50 K and significantly above 200 K in the dark. In this process, the structural change produced at 10 K, which is limited in the region close to the FAD chromophore, seems to induce further conformational change that is allowed only at higher temperatures. On the other hand, the F form was produced in less than 10 ns at room temperature. The transient absorption measurement in the present study did not detect the triplet state of flavin, which is known to exhibit bleaching at around 450 nm and gives a new absorption band at around 660 nm (24–26). The photoconversion process of the Tll0078 protein, therefore, does not include the long-lived triplet state of FAD, in contrast to the photocycle of the LOV domain (24, 26).

On the basis of the results in the present study, the photocycle of the BLUF protein at room temperature seems to proceed as follows: (i) FAD in the dark-adapted D form is photoexcited to the singlet excited state FAD\*; (ii) FAD\* relaxes to FAD in parallel with the formation of the 5-nm-shifted I with a time constant at around 0.12 ns, which occurs with a tiny alteration of the molecular coordinates of flavin and atoms of amino acid side chains to give a modification of H-bond to isoalloxazine C=O of FAD; (iii) the I form converts into the 10-nm-shifted F form in less than 10 ns forming the stronger H-bond due to the larger change of protein structure; and then (iv) F recovers to the D form again with a  $\Delta G^\ddagger$  of 0.84 eV accompanied by the change of protein structure. At temperatures lower than 50 K, the conversion process (iii) stops. However, we did not detect 5-nm-shifted I at 290 K in a time range longer than 10 ns after laser excitation; therefore, it is also probable that either the rate of process iii is comparable or faster than that of ii or that the F form is directly formed from FAD\* at higher temperatures.

The photocycle seems to include the modification of H-bond mainly to the isoalloxazine C(4)=O group as recently suggested by Hasegawa et al. on the basis of the FTIR measurement of the Slr1694 protein in the temperature range between 230 and 290 K (19). The transition from the F to the D form that accompanies the high activation energy change is known to slow down in D<sub>2</sub>O in the case of Slr1694 (18).

**Efficiency and Reversibility of the Photocycle.** Annealing experiments gave more insights into the photocycle. The illumination at 10 K produced I in one-half of the proteins after prolonged illumination, although the reason for the 50% efficiency of this step is unclear. The I-to-F form transition occurs partially at 50–200 K and fully above 200 K. Above 200 K, one-half of I turned to the F form and the other half returned to the D form. The reason for the 50% efficiency of the I to F form conversion is again unclear. The low efficiency is rather strange, since F formed by illumination above 200 K, once formed, never returned to the D form below 270 K, as seen from the temperature dependency in Figure 2. It can be said that the I form is less stable than the D form. Altogether, about 1/4 of the total protein yielded the F form after sufficiently long illumination at 10 K and

subsequent annealing at 240 K. This overall yield is almost comparable to the 29% apparent quantum efficiency of the F form estimated in the experiment under continuous illumination at room temperature. The apparent coincidence of the “overall yield after the 10 K illumination” and the “quantum efficiency at room temperature” may indicate that I is an intermediate in the whole photocycle rather than a byproduct in a side path. Further studies, however, will be required to fully evaluate the efficiencies of the photocycle at room temperature and at low temperatures. Time-resolved absorption spectroscopy in a time range faster than 10 ns is required to understand the reaction mechanism at room temperature, although the slow F to D form recovery rate of the protein makes these measurements rather difficult at present.

The fluorescence of FAD in aqueous solution, in which the isoalloxazine ring is unstacked with adenine, is known to exhibit a 3-ns decay time at room temperature (27, 28). Therefore, the measured 0.12 ns lifetime in this study suggests a competing quenching process that is more than 10 times faster than the intrinsic lifetime. If the competing process is the initial step of the photoconversion, an expected quantum efficiency of the initial step should be more than 90%. The initial photochemical process would occur from the photoexcited singlet state of flavin, since no triplet state was detected in the present measurement, although the participation of the triplet state with a very high turnover rate cannot be excluded. On the other hand, the “overall yield” or “quantum efficiency at room temperature” was 29%, as estimated above, indicating that some dissipation process competes against the FAD\*-to-I or the I-to-F form transition process even at room temperature.

We determined the activation energy of the reaction from the F to the D form to be 840 meV (81 kJ/mol) at 320 K. The time constants of this reaction at 320 and 293 K are 1.7 and 16 s, respectively. AppA was reported to give a 15-min recovery half-time ( $\tau_{1/e} \sim 20$  min) (4). Tll0078, thus, has a recovery rate that is about 80-fold faster than that of AppA in comparisons at room temperature. The ratio becomes 700-fold when the comparisons are made at the growth temperatures of the two organisms. The difference may indicate different functions or mechanisms of the photocycles of these proteins.

The activation enthalpy and entropy of the transition from I to F were calculated to be 5.7 meV (0.55 kJ/mol) and  $-3.4$  meV K<sup>-1</sup> ( $-0.33$  kJ mol<sup>-1</sup> K<sup>-1</sup>), respectively, from the variation of the population of I after annealing below 240 K (see Appendix for the details). The values for the transition from I to D, on the other hand, were calculated to be 290 meV (27 kJ mol<sup>-1</sup>) and  $-1.8$  meV K<sup>-1</sup> (0.17 kJ mol<sup>-1</sup> K<sup>-1</sup>), i.e., with a significantly larger activation enthalpy. The results suggest that the rearrangement of the pigment-protein structure is larger for the backward I-to-D transition than the forward I-to-F transition. The rates of transitions from I to F and from I to D can, then, be calculated to be  $3.8 \times 10^{-5}$  s<sup>-1</sup> and  $7.3 \times 10^{-2}$  s<sup>-1</sup>, respectively, if we extrapolate to 290 K. The forward I-to-F transition rate, therefore, will be one-thousandth of that of the backward I-to-D transition rate at 290 K based on the result of a dark annealing experiment. It is surprising that this calculation predicts “no formation of the F state at room temperature” and cannot interpret the observed “high 29% quantum efficiency”.

Therefore, the discrepancy may indicate a somewhat different mechanism of protein conformation changes at low and high temperatures. This may come from the different movements of protein structure in water and in ice or the variation of the rate-limiting activation process at the high-temperature regions. At room temperature, it is also probable that the rate of the I-to-F transition is faster than that of the FAD\*-to-I transition.

*Heterogeneity of the Dark-Adapted State.* The illumination at 10 K produced I in only one-half of the proteins. The result suggests low efficiency due to some recovery process or the existence of an inactive protein fraction. The recovery rate from I to D was negligible at 10 K, and the extent of photoconversion did not increase even after longer or higher-intensity illumination at 10 K. The results, thus, seem to indicate the heterogeneity of the protein, although the spectrum of FAD in the D form seemed homogeneous. The yield increased to almost unity above 270 K, as shown in Figure 2B. The results indicate the importance of dynamic equilibration of the protein structure and suggest that a tiny thermal fluctuation of the protein structure close to the FAD is essential for the initial photoconversion process.

*Mechanism of the Photoconversion.* Factors inducing spectral changes of flavin-binding enzymes or sensory proteins can be grouped into four types: (i) hydrophobic property around the chromophore (29), (ii) H-bond between flavin and polar amino acid residues (10, 18, 19, 30–32), (iii) interaction between the molecular orbitals of the isoalloxazine ring of the flavin and the aromatic rings of amino acid residues (10), and (iv) (de-)protonation of the isoalloxazine ring of the flavin (11). Masuda et al. reported a light-induced low-energy shift of C(2)=O and C(4)=O stretching vibrational modes of the isoalloxazine ring based on the FTIR spectroscopy of Slr1694 protein of *Synechocystis* sp. PCC6803 (18, 19). They proposed a conversion process that includes modifications of the H-bonds between FAD and protein. A similar reasoning might be applied to interpret the results in the present study since the modification of the H-bond of carbonyl will shift the FAD spectrum. However, the I form detected in this study seems to be different from the intermediate structure detected by FTIR at 230 K. The latter study covered a temperature range only above 230 K and did not detect the 5-nm-shifted form.

It is interesting that the Tll0078 protein transmits the signal to the receptor proteins. The deletion of the slr1694 gene has changed the direction of phototaxis in *Synechocystis* PCC6803 (16, 17). It has been reported that hydrogen bonding of riboflavin increases the electrophilicity of the excited state of the flavin (33). It is now clear that the I form, which can be formed only at 10 K, has only a slight structural change in the close vicinity of flavin compared to the D form. The structural change, then, propagates inside the protein with large changes in enthalpy and entropy through the I-to-F transition above 200 K. Further conformational change might also occur after transition to F. The conformational change with a slight movement of H atom(s) close to the flavin seems to trigger the initial step of the photoconversion of BLUF protein.

## APPENDIX

The values of the activation enthalpy and entropy of the transition from I to F and from I to D were estimated by the



temperature-dependent change of the population ( $c_1$ ) of the I form after the annealing treatment shown in Figure 7. If we assume that I can relax into either D or F, the rate of the change of  $c_1$  can be expressed as the function of  $c_1$  as well as  $k_{IF}$  and  $k_{ID}$ , which are the temperature-dependent rate constants for the reactions from I to F and to D, respectively (eq 1).

$$\frac{dc_1(T(t))}{dt} = -(k_{IF} + k_{ID})c_1(T(t)) \quad (1)$$

$$\begin{cases} k_{IF} = k_{IF}^0 \exp\left(-\frac{\Delta G_{IF}^\ddagger}{k_B T(t)}\right) \\ k_{ID} = k_{ID}^0 \exp\left(-\frac{\Delta G_{ID}^\ddagger}{k_B T(t)}\right) \end{cases}$$

$k_{IF}$  and  $k_{ID}$  are also related to the activation energies,  $\Delta G_{IF}^\ddagger$  and  $\Delta G_{ID}^\ddagger$ , of the reactions from I to F and I to D, respectively.  $k_B$  and  $T(t)$  represent the Boltzmann constant and sample temperature, respectively.  $c_1$  after each annealing treatment, then, could be obtained by integrating eq 1 over time.

$$c_1(T(t)) = c_1(10K) \exp\left(\int_0^t -k_{IF}^0 \exp\left(-\frac{\Delta G_{IF}^\ddagger}{k_B T(t')}\right) - k_{ID}^0 \exp\left(-\frac{\Delta G_{ID}^\ddagger}{k_B T(t')}\right) dt'\right) \quad (2)$$

$$\cong c_1(10K) \exp\left(\sum_i^n \left(-k_{IF}^0 \exp\left(-\frac{\Delta G_{IF}^\ddagger}{k_B T_i}\right) - k_{ID}^0 \exp\left(-\frac{\Delta G_{ID}^\ddagger}{k_B T_i}\right)\right) (\Delta t)\right) \quad (3)$$

$$c_1(T_n) = c_1(10K) \prod_i^n \left(\exp\left(-k_{IF}^0 \exp\left(-\frac{\Delta G_{IF}^\ddagger}{k_B T_i}\right) - k_{ID}^0 \exp\left(-\frac{\Delta G_{ID}^\ddagger}{k_B T_i}\right)\right) (\Delta t)\right) \quad (4)$$

In this case, the initial condition for the integration was determined by the population  $c_1$  of the I form measured at 10 K. The integration was replaced by the summation in eq 3 by assuming that the reactions occurred in the meantime ( $\Delta t$ ) at the elevated temperature  $T_i$  at each annealing process. The value of  $\Delta t$  was set to 20 min in the present experiment. The  $T_i$  values used were 50, 100, 150, 200, and 240 K. From eq 4, we can calculate the relative change of  $c_1$  after the annealing process as follows:

$$\frac{c_1(T_n)}{c_1(T_{n-1})} = \exp\left(\left(-k_{IF}^0 \exp\left(-\frac{\Delta G_{IF}^\ddagger}{k_B T_n}\right) - k_{ID}^0 \exp\left(-\frac{\Delta G_{ID}^\ddagger}{k_B T_n}\right)\right) (\Delta t)\right) \quad (5)$$

The logarithm of the ratio of  $c_1(T_n)/c_1(T_{n-1})$  was plotted against  $1/T$  (data not shown), and the activation energy of

the transitions was calculated. The values of the activation enthalpy and entropy of the reaction from the I to the F form were calculated to be 5.7 meV and  $-3.4$  meV/K, respectively. The values for the transition from I to D, on the other hand, were calculated to be 290 meV and  $-1.8$  meV/K, i.e., with a significantly larger activation enthalpy.

## ACKNOWLEDGMENT

The authors thank Dr. H. Mino for his valuable discussion during the study. Thanks are also due to Drs. S. Masuda and T. Ono in Riken and to Dr. T. Noguchi of Tsukuba University for their helpful suggestions.

## REFERENCES

1. van der Horst, M. A., and Hellingwerf, K. J. (2004) Photoreceptor proteins, "star actors of modern times": a review of the functional dynamics in the structure of representative members of six different photoreceptor families, *Acc. Chem. Res.* 37, 13–20.
2. Braatsch, S., and Klug, G. (2004) Blue light perception in bacteria, *Photosynth. Res.* 79, 45–57.
3. Crosson, S., Rajagopal, S., and Moffat, K. (2003) The LOV domain family: Photoresponsive signaling modules coupled to diverse output domains, *Biochemistry* 42, 2–10.
4. Masuda, S., and Bauer, C. E. (2002) AppA is a blue light photoreceptor that antirepresses photosynthesis gene expression in *Rhodobacter sphaeroides*, *Cell* 110, 613–623.
5. Giovani, B., Byrdin, M., Ahmad, M., and Brettel, K. (2003) Light-induced electron transfer in a cryptochrome blue-light photoreceptor, *Nat. Struct. Biol.* 10, 489–490.
6. Gomelsky, M., and Kaplan, S. (1995) appA, a novel gene encoding a *trans*-acting factor involved in the regulation of photosynthesis gene expression in *Rhodobacter sphaeroides* 2.4.1, *J. Bacteriol.* 172, 4609–4618.
7. Gomelsky, M., and Kaplan, S. (1997) Molecular genetic analysis suggesting interactions between AppA and PpsR in regulation of photosynthesis gene expression in *Rhodobacter sphaeroides* 2.4.1, *J. Bacteriol.* 179, 128–134.
8. Gomelsky, M., and Kaplan, S. (1998) AppA, a redox regulator of photosystem formation in *Rhodobacter sphaeroides* 2.4.1, is a flavoprotein, *J. Biol. Chem.* 273, 35319–35325.
9. Braatsch, S., Gomelsky, M., Kuphal, S., and Klug, G. (2002) A single flavoprotein, AppA, integrates both redox and light signals in *Rhodobacter sphaeroides*, *Mol. Microbiol.* 45, 827–836.
10. Kraft, B. J., Masuda, S., Kikuchi, J., Dragnea, V., Tollin, G., Zaleski, J. M., and Bauer, C. E. (2003) Spectroscopic and mutational analysis of the blue-light photoreceptor AppA: a novel photocycle involving flavin stacking with an aromatic amino acid, *Biochemistry* 42, 6726–6734.
11. Laan, W., van der Horst, M. A., van Stokkum, I. H., and Hellingwerf, K. J. (2003) Initial characterization of the primary photochemistry of AppA, a blue-light-using flavin adenine dinucleotide-domain containing transcriptional antirepressor protein from *Rhodobacter sphaeroides*: a key role for reversible intramolecular proton transfer from the flavin adenine dinucleotide chromophore to a conserved tyrosine?, *Photochem. Photobiol.* 78, 290–297.
12. Masuda, S., Hasegawa, K., and Ono, T. (2005) Light-induced structural changes of apoprotein and chromophore in the sensor of blue light using FAD (BLUF) domain of AppA for a signaling state, *Biochemistry* 44, 1215–1224.
13. Han, Y., Braatsch, S., Osterloh, L., and Klug, G. (2004) A eukaryotic BLUF domain mediates light-dependent gene expression in the purple bacterium *Rhodobacter sphaeroides* 2.4.1, *Proc. Natl. Acad. Sci. U.S.A.* 101, 12306–12311.
14. Gomelsky, M., and Klug, G. (2002) BLUF: a novel FAD-binding domain involved in sensory transduction in microorganisms, *Trends Biochem. Sci.* 27, 497–500.
15. Iseki, M., Matsunaga, S., Murakami, A., Ohno, K., Shiga, K., Yoshida, K., Sugai, M., Takahashi, T., Hori, T., and Watanabe, M. (2002) A blue-light-activated adenylyl cyclase mediates photoavoidance in *Euglena gracilis*, *Nature* 415, 1047–1051.
16. Okajima, K., Yoshihara, S., Geng, X., Katayama, M., and Ikeuchi, M. (2003) Structural and functional analysis of a novel flavo-protein in cyanobacteria, *Plant Cell Physiol.* 44 (Suppl), 162.

17. Masuda, S., and Ono, T. (2004) Biochemical characterization of the major adenylyl cyclase, Cya1, in the cyanobacterium *Synechocystis* sp. PCC 6803, *FEBS Lett.* 577, 255–258.
18. Masuda, S., Hasegawa, K., Ishii, A., and Ono, T. (2004) Light-induced structural changes in a putative blue-light receptor with a novel FAD binding fold sensor of blue-light using FAD (BLUF); Slr1694 of *Synechocystis* sp. PCC6803, *Biochemistry* 43, 5304–5313.
19. Hasegawa, K., Masuda, S., and Ono, T. (2004) Structural intermediate in the photocycle of a BLUF (sensor of Blue Light Using FAD) protein Slr1694 in a cyanobacterium *Synechocystis* sp. PCC6803, *Biochemistry* 43, 14979–14986.
20. Hellingwerf, K. J., Hendriks, J., and Gensch, T. (2003) Photoactive yellow protein, a new type of photoreceptor protein: Will this “yellow lab” bring us where we want to go?, *J. Phys. Chem. A* 107, 1082–1094.
21. Hellingwerf, K. J. (2000) Key issues in the photochemistry and signalling-state formation of photosensor proteins, *J. Photochem. Photobiol., B* 54, 94–102.
22. Studier, F. W., Rosenberg, A. H., Dunn, J. J., and Dubendorff, J. W. (1990) Use of T7 RNA polymerase to direct expression of cloned genes, *Methods Enzymol.* 185, 60–89.
23. Akmal, A., and Muñoz, V. (2004) The nature of the free energy barriers to two-state folding, *Proteins* 57, 142–152.
24. Kennis, J. T. M., Crosson, S., Gauden, M., van Stokkum, I. H. M., Moffat, K., and van Grondelle, R. (2003) Primary reactions of the LOV2 domain of phototropin, a plant blue-light photoreceptor, *Biochemistry* 42, 3385–3392.
25. Schreiner, S., Steiner, U., Kramer H. E. A. (1975) Determination of the pK values of the lumiflavin triplet state by flash photolysis, *Photochem. Photobiol.* 21, 81–84.
26. Swartz, T. E., Corchnoy, S. B., Christie J. M., Lewis, J. W., Szundi, I., Briggs, W. R., and Bogomolni, R. A. (2001) The photocycle of a flavin-binding domain of the blue light photoreceptor phototropin, *J. Biol. Chem.* 276, 36493–36500.
27. Visser, A. J. W. G. (1984) Kinetics of stacking interactions in flavin adenine dinucleotide from time-resolved flavin fluorescence, *Photochem. Photobiol.* 40, 703–706.
28. Islam, S. D. M., Susdorf, T., Penzkofer, A., and Hegemann, P. (2003) Fluorescence quenching of flavin adenine dinucleotide in aqueous solution by pH dependent isomerisation and photo-induced electron transfer, *Chem. Phys.* 295, 137–149.
29. Stanley, R. J., and Siddiqui, M. S. (2001) A stark spectroscopic study of *N*(3)-methyl, *N*(10)-isobutyl-7,8-dimethylisalloxazine in nonpolar low-temperature glasses: experiment and comparison with calculations, *J. Phys. Chem. A* 105, 11001–11008.
30. Gopalan, K. V., and Srivastava, D. K. (2002) Beyond the proton abstracting role of Glu-376 in medium-chain acyl-CoA dehydrogenase: influence of Glu-376→Gln substitution on ligand binding and catalysis, *Biochemistry* 41, 4638–4648.
31. Koziol, J., and Szafran, M. M. (1990) Spectral properties of riboflavin tetrabutylate in the presence of hydrogen-bonding agents, *J. Photochem. Photobiol., B* 5, 429–443.
32. Nishimoto, K., Watanabe, Y., and Yagi, K. (1978) Hydrogen bonding of flavoprotein, *Biochim. Biophys. Acta* 526, 34–41.
33. Heelis, P. F., and Koziolowa, A. (1991) The effect of hydrogen bonding on the electron transfer reactions of the excited singlet and triplet states of flavins, *J. Photochem. Photobiol., B* 11, 365–370.

BI048044Y